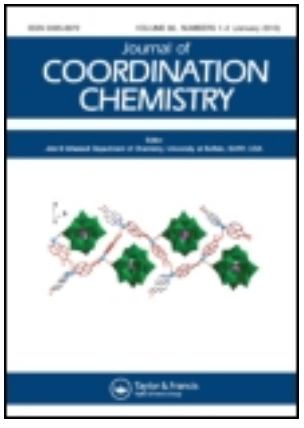

Journal of Coordination Chemistry
Publication details, including instructions for authors and subscription information:
http://www.tandfonline.com/loi/gcoo20

An easy synthesis of nanostructured magnetite-loaded functionalized carbon spheres and cobalt ferrite

Ali M. Hassan[a], Amr M. Nassar[a], Nabila M. Ibrahim[b], Ahmed M. Elsaman[c] & Mohamed M. Rashad[c]

[a] Deparment of Chemistry, Faculty of Science, Al-Azhar Univeristy, Cairo, Egypt

[b] Department of Organometallic & Organometalloid Chemistry, National Research Centre, Cairo, Egypt

[c] Department of Advanced Materials, Central Metallurgical Research & Development Institute (CMRDI), Cairo, Egypt

Published online: 10 Dec 2013.

To cite this article: Ali M. Hassan, Amr M. Nassar, Nabila M. Ibrahim, Ahmed M. Elsaman & Mohamed M. Rashad (2013) An easy synthesis of nanostructured magnetite-loaded functionalized carbon spheres and cobalt ferrite, Journal of Coordination Chemistry, 66:24, 4387-4398, DOI: 10.1080/00958972.2013.867037

To link to this article: http://dx.doi.org/10.1080/00958972.2013.867037

Journal of Coordination Chemistry, 2013
Vol. 66, No. 24, 4387–4398, http://dx.doi.org/10.1080/00958972.2013.867037

An easy synthesis of nanostructured magnetite-loaded functionalized carbon spheres and cobalt ferrite

ALI M. HASSAN†, AMR M. NASSAR†, NABILA M. IBRAHIM‡, AHMED M. ELSAMAN*§ and MOHAMED M. RASHAD§

†Deparment of Chemistry, Faculty of Science, Al-Azhar Univeristy, Cairo, Egypt
‡Department of Organometallic & Organometalloid Chemistry, National Research Centre, Cairo, Egypt
§Department of Advanced Materials, Central Metallurgical Research & Development Institute (CMRDI), Cairo, Egypt

(*Received 2 August 2013; accepted 13 November 2013*)

An easy method in a solvothermal system has been developed to synthesize nanostructured magnetite (Fe_3O_4)-loaded functionalized carbon spheres (CSs) and cobalt ferrite ($CoFe_2O_4$). Surface-tunable CSs loaded with iron oxide (Fe_3O_4) nanoparticles were prepared using an acetylferrocene Schiff base (OPF), whereas spinel cobalt ferrite ($CoFe_2O_4$) was synthesized via metal complexes of a ferrocenyl Schiff base with phenol moiety (Co-OPF). The formed composite powder was investigated using X-ray powder diffraction, Raman spectrometry, Fourier transform infrared spectroscopy, scanning electron microscopy, energy-dispersive X-ray spectroscopy, and vibrating sample magnetometry. It was found that most of the iron oxide nanoparticles were evenly distributed upon the surface of the CSs. Furthermore, the surface of the iron oxide-loaded CSs has large numbers of functional groups. Good saturation magnetization was achieved for the formed magnetic nanoparticles.

Keywords: Nanostructures; Organometallic compounds; Magnetic material; Magnetite-loaded carbon sphere

1. Introduction

Iron oxide nanoparticles are employed in numerous environmental applications including Fischer–Tropsch catalysts, oxygen reduction catalysts in fuel cells, environmental adsorbents for CO or arsenic, catalysts for CO oxidation, and destruction of polychlorinated dibenzodioxins/dibenzofurans PCDDs/PCDFs [1–4]. Surface modification and/or coating of carbon spheres (CSs) have been of considerable interest recently. Coating the CSs with metal, alloy, oxide, or semiconductor nanoparticles could improve the functionality, compatibility, and reactivity of the surface. Therefore, spheres with specific catalytic, magnetic, electronic, optical, or optoelectronic properties have greatly widened their utility in the fields of electronics, magnetism, optics, catalysis, and bioscience [5–11]. Carbon provides several advantages as a metal nanoparticle support including inertness in acidic and basic conditions, thermal and mechanical stability of the porous structure, and high surface area

*Corresponding author. Email: a.m.elsaman@cmrdi.sci.eg

and defined/modifiable porous structure [12]. For example, Wang *et al.* [13] fabricated ZnO nanoparticles and nanorods coated on CS surfaces. The results were observed in all products.

Metal-impregnated carbon materials are traditionally prepared in a multi-step process which includes selection, preparation, and modification of the carbon support; loading of the metal precursor onto carbon using incipient wetness, excess solution, ion-exchange impregnation techniques, or chemical vapor deposition; and conversion of the metal precursor to the desired metal oxide or zero-valent form by physical (e.g. heating) or chemical (e.g. reduction) treatments [14]. Therefore, a continuous, single-step process is developed for preparing nanostructured porous CSs impregnated with magnetite (Fe_3O_4) or zero-valent iron nanoparticles (Fe–C) from ferrocenyl derivatives. In addition, Fe_3O_4, as a conventional magnetic material, has shown great potential applications in targeted drug delivery, protein separation, magnetic recording media, and magnetic resonance imaging (MRI) [15, 16].

The objective of the present work is to describe the synthesis of the magnetite-loaded CS products. By means of a solvothermal route, the proposed mechanism for their formation is investigated. On the other hand, it is not easy to coat the CSs with other functional materials, especially in one step. Here an easy method is reported to synthesize iron oxide-loaded functionalized CSs and cobalt ferrite ($CoFe_2O_4$). Then the complex is employed as composite precursor for synthesis of $CoFe_2O_4$. Experiments were carried out using ethylene glycol (EG), which has been reported as an effective reaction medium due to its special physical and chemical properties [17–19].

2. Experimental

2.1. *Materials*

Acetylferrocene was obtained from Sigma Aldrich Chemical Co. and used directly without further purification. All other reagents were of analytical grade.

2.2. *Methods*

2.2.1. Synthesis of Fe_3O_4-loaded CSs. The OPF was synthesized first by dissolving 2-aminophenol (1.09 g, 10 mM) in about 20 mL ethylacetate; then, the formed solution was added slowly to a magnetically stirred solution of acetylferrocene (2.28 g, 10 mM) in 20 mL ethylacetate. The mixture was refluxed for 2 h. The solution was concentrated to the appropriate volume. Thereafter, it was cooled at 5 °C, filtered, treated with ethanol solution, and dried overnight. Then the purity of products was checked by thin layer chromatography (TLC) on silica gel. The product obtained was recrystallized from 10 to 15 mL hot ethanol to give OPF. Chemical Formula of OPF: $C_{18}H_{17}FeNO$ which is illustrated in figure 1.

Then, 0.3 g of OPF was dispersed in EG (10 mL) with water (5 mL) with the aid of ultrasonication at room temperature to form a suspension. The resulting suspension was sealed in a 25 mL Teflon-lined stainless steel (autoclave) and maintained at 160 °C for 24 h, and then cooled to room temperature naturally. The black products were separated by centrifugation, washed several times with deionized water, absolute ethanol, and acetone, and then dried under vacuum at room temperature.

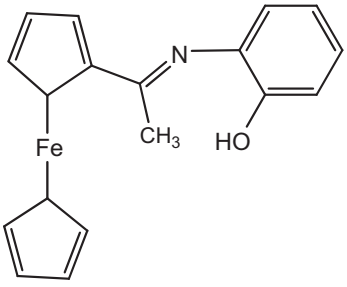

Figure 1. Suggested structure of OPF.

2.2.2. Synthesis of $CoFe_2O_4$. The complexes were prepared by adding 2.0 mM of $CoCl_2 \cdot 6H_2O$ (dissolved in ca. 20 mL water) in a warmed solution of the ligand (4.0 mM of OPF) in ethanol (20 mL). The mixture was refluxed for 2.0 h. The complex that separated out on cooling at 5 °C was filtered, washed twice with cold ethanol, and dried. Chemical formula of Co (OPF): $C_{36}H_{36}CoFe_2N_2O_4$. The suggested structure is shown in figure 2.

The cobalt ferrite synthesized from Co (OPF) was dispersed in (10 mL) water with the aid of ultrasonication at room temperature to form a suspension. The resulting suspension was autoclaved and maintained at 250 °C for 24 h, and then cooled to room temperature naturally. The black products were separated by centrifugation, washed several times with deionized water, absolute ethanol, and acetone, and then dried under vacuum at room temperature.

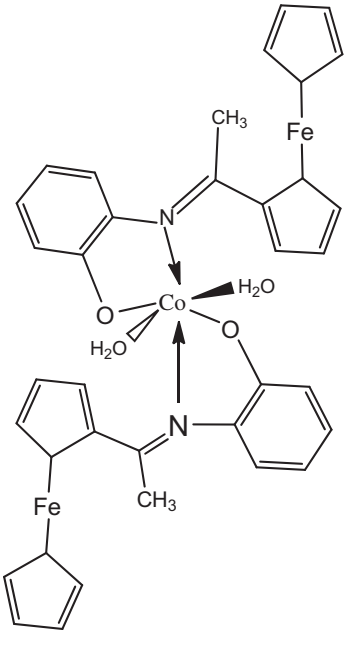

Figure 2. Suggested structure of Co (OPF).

2.3. *Physical characterization*

The as-prepared products were characterized using an ultrasonic generator (Dr Hielscher UP400 S ultrasonic processor) equipped with an H22 sonotrode of 22 mm diameter, operating at 24 kHz with a maximum power output of 400 W, for the ultrasonic irradiation. The ultrasonic generator automatically adjusts the power level. X-ray powder diffraction (XRD) was identified using a Bruker D8-advance (Cu Kα λ = 0.154056 nm). Scanning electron microscopy (SEM) was performed using a Philips XL-30E. FT-IR and Raman Spectroscopy were compressed with KBr as disks on the JASCO FT/IR-6300 type A spectrometer. Magnetic measurements were measured using a vibrating sample magnetometer (VSM; Lake Shore, 7600 LDJ, USA) in a maximum applied field of 10 kOe. From the obtained hysteresis loops, the saturation magnetization (M_s), remanence magnetization (M_r), and coercive field (H_c) were determined.

3. Results and discussion

In this paper, the Fe_3O_4 nanoparticle-loaded CSs were obtained by adding EG from the OPF Schiff base to the reaction medium. The structure and the chemical composition of the products were determined by XRD. The pattern (figure 3(a)) indicates that the spinel structure has two cations sites: the tetrahedrally coordinated A sites and the octahedrally coordinated B sites. For Fe_3O_4, the A and B positions are occupied by Fe^{3+} and Fe^{2+} cations, respectively. For $CoFe_2O_4$, the A and B positions are equally occupied by Co and Fe cations. Fe_3O_4 and $CoFe_2O_4$ have an almost similar lattice parameter: a = 8.3963 Å for Fe_3O_4, a = 8.39 Å for $CoFe_2O_4$.

To investigate the effect of experimental parameters on the formation of the products, a series of experiments was carried out: first, using EG with water at 160 °C for 24 h to give Fe_3O_4-loaded CSs, and second using 10 mL water at 160 °C for 24 h to produce Fe_3O_4

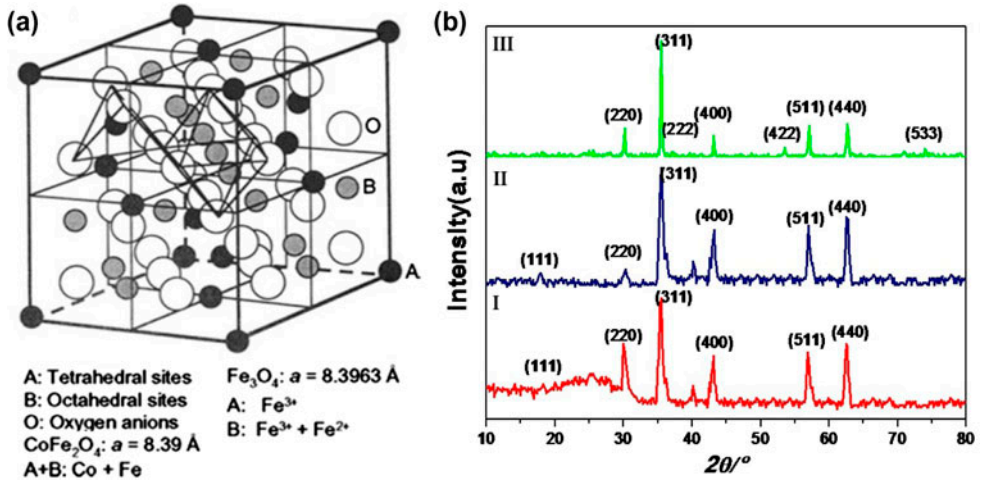

Figure 3. (a) Schematic model of the spinel unite cell structure and (b) XRD patterns of: (I) Fe_3O_4-loaded CSs and (II) Fe_3O_4 (III) $CoFe_2O_4$-loaded CSs.

only. It is well known that water can serve as a solvent in the liquid phase reaction. Therefore, the Fe_3O_4 nanoparticles were obtained without CSs by adding water to the reaction medium and decomposition of carbon and nitrogen present in chemical constituent of the Schiff base ligand (OPF) due to the higher temperature of the hydrothermal system than the boiling point of water, while in the synthesized Fe_3O_4-loaded CSs the solvothermal system is 160 °C lower than the boiling point of EG. So, EG has a higher viscosity than water, increases the viscosity of the reaction medium, and then decreases the diffusion rate of solutes, thus resulting in the formation of CSs from carbon present in OPF. And it is well known that EG can serve as both a solvent and a reducing agent in the liquid phase reaction [20–23]. Figure 3(b) (I, II) displays the XRD pattern of the Fe_3O_4 nanoparticles, which can be indexed to the Fe_3O_4 phase with lattice parameter a = 8.398 Å (JCPDS 19-0629). This presents further evidence of the formation of Fe_3O_4. Moreover, a weak and broad peak at around $2\theta = 25°$ was observed in the XRD pattern of Fe_3O_4-loaded CSs figure 3(b) (I) indicates an amorphous structure of the CSs.

The $CoFe_2O_4$ can be synthesized from the Co complex of OPF in 10 mL water at 250 °C for 24 h in the hydrothermal system Also, the decomposition of C and N in the system happens by the higher temperature of reaction. In figure 3(b) (III), the resolved diffraction peaks can be indexed to $CoFe_2O_4$ phases which match the standard card of (JCPDS # 33-0664). The $CoFe_2O_4$ was synthesized via the cobalt complex Schiff base (Co-OPF), while the characteristic peaks were observed for other impurities, such as α-Fe_2O_3, in $CoFe_2O_4$ only. The mass densities for Fe_3O_4 and $CoFe_2O_4$ (in figure 3(b) (I–III)) are almost identical. Considering the facts of the very small difference in atomic numbers between Co and Fe and the identical crystal structure, the two phases can be hardly distinguished by X-ray diffraction, especially with the shape-induced peak broadening [24].

Furthermore, the crystallite sizes of the produced magnetite nanoparticles loaded onto the CSs (I), magnetite (II), and $CoFe_2O_4$ (III) nanoparticles for the most intense peak (311) planes were calculated from the XRD data based on the Debye–Scherrer formula. It was found that the crystallite sizes of the formed powders were ~50, 65, and 86 nm, respectively.

The change in the microstructures of the formed powders was investigated using FESEM micrographs, as shown in figure 4. The formed particles consist of a large quantity of Fe_3O_4-loaded CSs and the CSs have perfect spheres with smooth surfaces with an average diameter of about 500 nm. It can be seen that the Fe_3O_4 nanoparticles loaded onto CSs are evenly distributed as small, round, and uniform white spots on the surface of the CSs. Moreover, it was found that some Fe_3O_4 nanoparticles are studded on the surface of the CSs. This special structure can effectively stabilize the Fe_3O_4 nanoparticles and prevent them from aggregation too. Additionally, the energy-dispersive X-ray spectroscopy (EDX) spectrum of the products indicates that the sample is mainly composed of Fe, O, and C, as given in figure 4(b).

Figure 5 displays the SEM image of Fe_3O_4 nanoparticles without CSs. It can be seen that the CSs become very low where there is the probability of the existence of a small percentage of carbon due to non-complete decomposition of carbon in the ligand, which may originate from the low-viscous solvent. Additionally, the EDX spectrum of the products indicates that the sample is mainly composed of Fe and O. The addition of water, which has lower viscosity than EG, decreases the viscosity of the reaction medium and then increases the diffusion rate of solutes.

Figure 6 demonstrates the SEM micrograph of $CoFe_2O_4$ nanoparticles. The particles appeared as very fine and homogeneous agglomerated grains. Additionally, the EDX

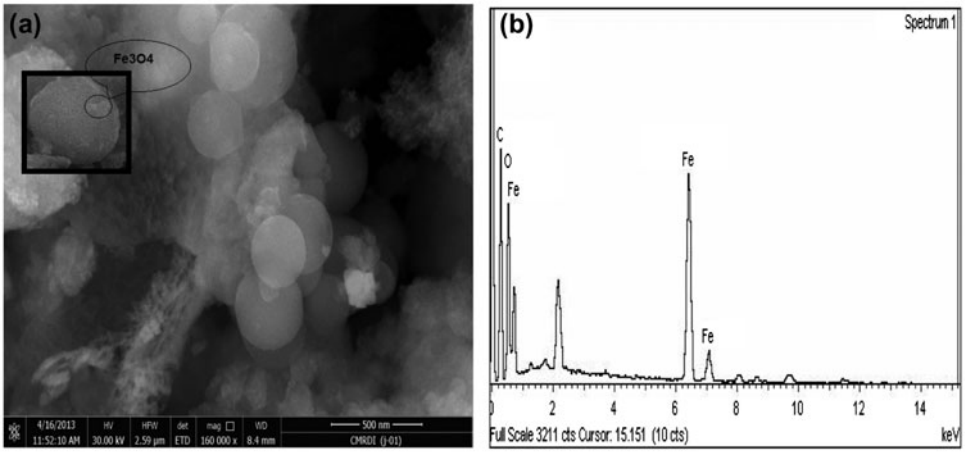

Figure 4. (a) FESEM and (b) EDX spectrum of magnetite-loaded CSs.

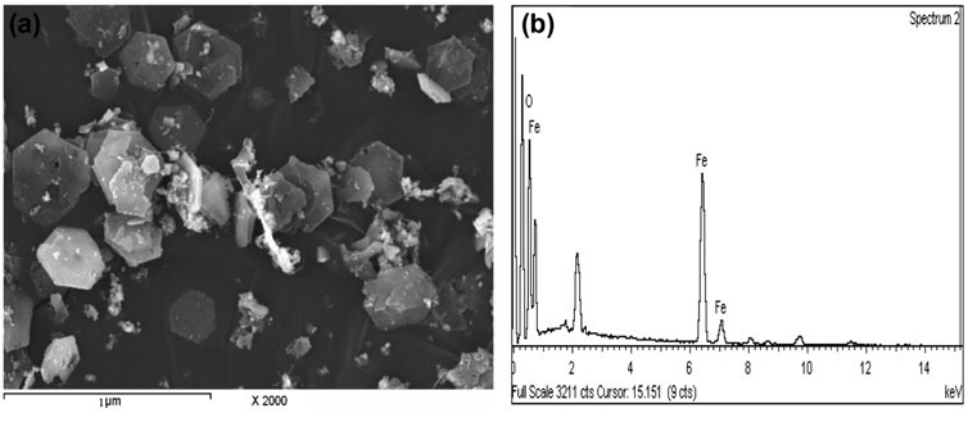

Figure 5. (a) SEM and (b) EDX of Fe_3O_4 without CSs (OPF 0.3 g, 10 mL water, 160 °C, 24 h).

spectrum of the products indicates that the sample is mainly composed of Co, Fe, and O, identical to the crystal structure of spinel $CoFe_2O_4$ phase. Furthermore, we indicate the quantitative analysis element. Table 1 shows the weight percent and intensity of Fe_3O_4–loaded CSs, Fe_3O_4, and $CoFe_2O_4$.

Raman and Fourier transform infrared spectroscopy (FT-IR) spectra were recorded to further disclose the structural nature of the products and the results are illustrated in figure 7. One can clearly see from figure 7(a) that peaks at the main band are centered at 668 cm^{-1} and peaks at ca. 540 cm^{-1} and 300 cm^{-1} have been assigned to A_{1g}, T_{2g}, and E_g vibrations of magnetite. These peak positions match that of typical Fe_3O_4 [25], which provides further support for the formation of the Fe_3O_4 phase. Prominent peaks in the Raman spectra at 1589 and 1350 cm^{-1} correspond to the E_{2g} (2) (G band) and disorder-induced (D band) modes of CSs, respectively. Broad bands at 2700–3200 cm^{-1} have been observed in the Raman spectra of both samples. Three bands at 2674, 2914, and 3181 cm^{-1} for carbon

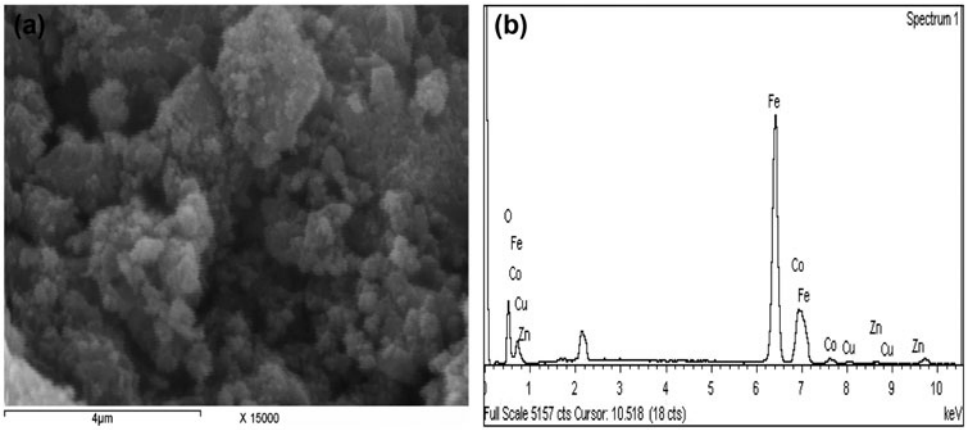

Figure 6. (a) SEM and (b) EDX spectrum of $CoFe_2O_4$.

Table 1. Quantitative analysis and intensity of Fe_3O_4-loaded CSs, Fe_3O_4, and $CoFe_2O_4$.

	Co		Fe		O		C	
	wt.%	Net inte.	wt.%	Net inte.	wt.%	Net inte.	wt.%	Net inte.
Fe_3O_4 loaded CSs	–		25.88	9994.64	42.99	584.61	31.14	2381.35
Fe_3O_4	–	–	42.44	1044.45	57.32	8765.34	–	–
$CoFe_2O_3$	15.22	343.76	29.35	2098.81	53.45	876.45	–	–

spheres (CSs) are obtained after spectral deconvolution (figure 7(a)). The bands at 2674 and 3181 cm^{-1} can be attributed, respectively, to the second-order D(2 χ D) and G(2 χ G) modes. The band at 2914 cm^{-1} is due to the combination mode of D and G bands [26]. Moreover, the FT-IR spectrum of the formed powders shown in figure 7(b) indicate that the peak at 592 cm^{-1} was attributed to the stretching vibration of Fe–O in Fe_3O_4 [27, 28]. Besides, a broad peak at 1060 cm^{-1} was ascribed to C–OH stretching vibration, whereas two bands around 1409 and 1595 cm^{-1} were observed, which can be assigned to the symmetric and asymmetric stretching vibration of COO– groups [29, 30]. All of those peaks revealed that the surface of the Fe_3O_4-loaded CSs still has large numbers of functional groups, such as C–OH and COO– groups, which makes surface modification unnecessary. Moreover, FT-IR spectra of the powders showed that the absorption bands at around 1140, 1620, and 2450 cm^{-1} are due to the stretching vibrations of the C–O and C=O, respectively. The broad band centered around 3400 cm^{-1} was related to anti-symmetric and symmetric vibration of the OH group of adsorbed water. Furthermore, it is observed that the absorption peak at 2930 cm^{-1} represents the stretching vibration of the C–H bond [31]. However, the FT-IR spectrum of $CoFe_2O_4$ has two main broad metal–oxygen bands as shown in figure 7(b). The highest one, generally observed in the range 600–500 cm^{-1}, corresponds to intrinsic stretching vibrations of the metal at the tetrahedral site Mtetra–O stretching vibration bands in $CoFe_2O_4$ compounds. A band observed at 731 cm^{-1} is assigned to the stretching mode of Co–O.

Based on the results, it was concluded that the Fe_3O_4-loaded CSs and $CoFe_2O_4$ have been synthesized through adding EG to the reaction medium. In addition, Fe_3O_4, as a conventional magnetic material, has shown great potential applications in targeted drug

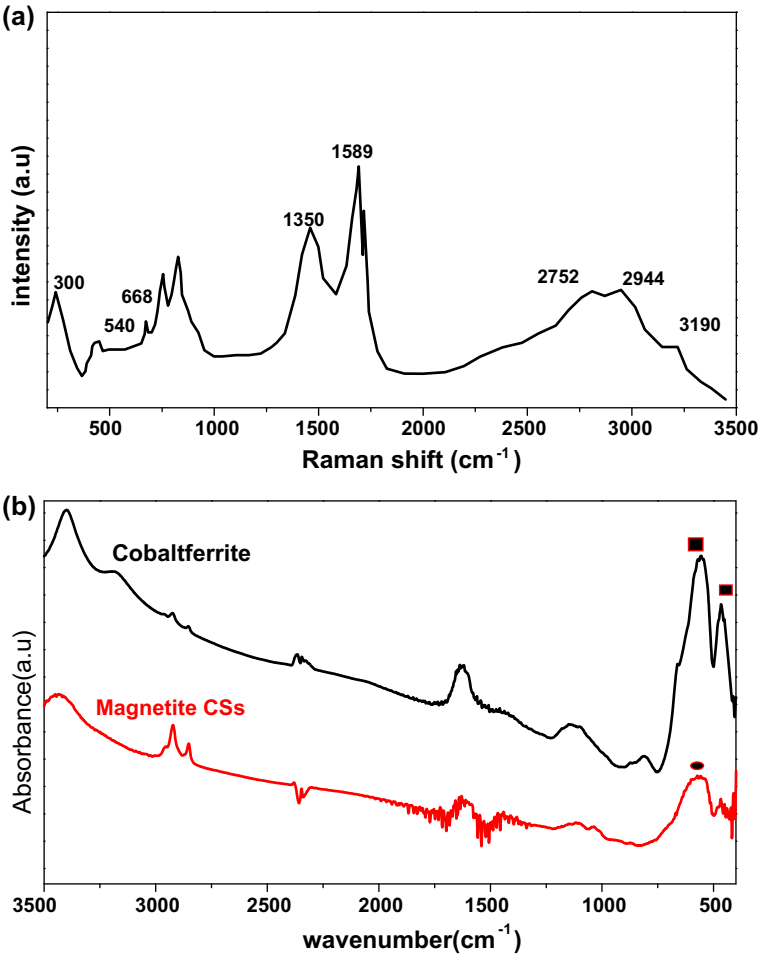

Figure 7. (a) Raman spectra of Fe_3O_4. (b) FT-IR spectra of Fe_3O_4-loaded CSs and $CoFe_2O_4$.

delivery, protein separation, magnetic recording media, and MRI, and also facilitates the absorption of metal ions using the composites as templates for multifunctional hybrid core/shell structures or hollow/porous composites.

Based on the results, it was concluded that the Fe_3O_4 without CSs has been synthesized through addition of water to the reaction medium. Taking into account the literature [13, 32–34] and our experimental results, a possible formation mechanism of the products is proposed, as schematically shown in figure 8, although the exact formation mechanism is not yet clear due to the reaction complexity in the sealed system. When the sealed reaction system was heated to a certain temperature, the precursor molecules in the solution started to dehydrate; some dehydrated compounds were formed during the initial stage. With the advancing of reaction, when the system reached a critical condition, the sphere nuclei were formed by the dehydrated compounds while the carbonization happened. Then, the resulting nuclei grew by diffusion of solutes to form CSs as driven by minimum interfacial energy. So, the formation of the CSs may follow dehydration or anhydridisation, nucleation,

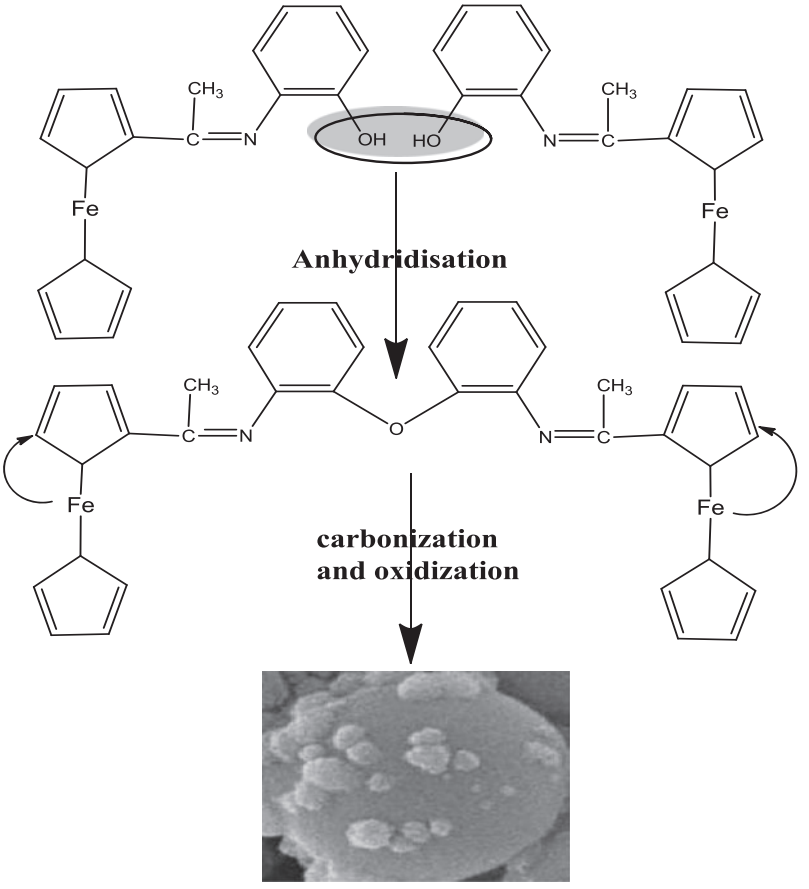

Figure 8. A schematic formation of Fe_3O_4-loaded CSs.

carbonization, and growth processes. At the same time, the Fe atoms reacted with the molecular water and residual oxygen dissolved in the solution to form FeOOH or $Fe(OH)_3$, and then the precursor accreted on the CSs was *in situ* dehydrated finally to form thermodynamically stable Fe_3O_4 particles in the sealed system. However, in the mixed solution, the EG acted as a reducing agent, which limited the oxidation degree of Fe atoms and promoted the formation of the Fe_3O_4 particles. As expected, EG plays an important role in the formation of the Fe_3O_4 particles.

It is of great interest to investigate the magnetic properties of Fe_3O_4-loaded CSs, Fe_3O_4, and $CoFe_2O_4$. The magnetic properties of the samples were investigated using a VSM with an applied field of 10 kOe. Figure 9 shows *M–H* hysteresis loops for the prepared samples measured at room temperature. The saturation magnetization (M_s) was 48.9, 35.3, and 36.1 emu/g whereas the coercivity force was, 12.0, 115.8, and 1189.9 Oe for Fe_3O_4-loaded CSs, Fe_3O_4, and $CoFe_2O_4$, respectively, as shown in table 1. The obtained values are lower than the bulk Fe_3O_4 value (M_s = 92 emu/g) [35, 36] and they are equal to the previously reported value by Hu *et al.* which was 48 emu/g [37]. Magnetic properties of materials are generally influenced by many factors, such as size, structure, surface disorder, morphologies, shape anisotropy, etc. [38, 39]. Furthermore, the M_s values were dependent on magnetite particle

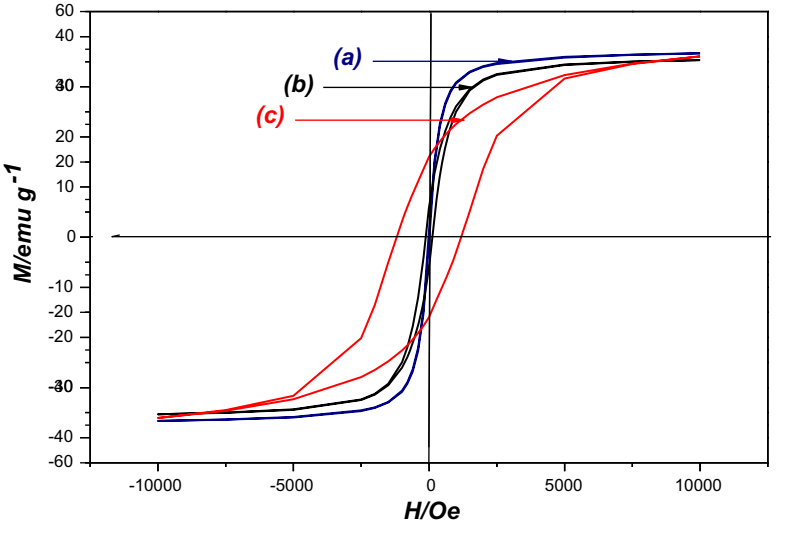

Figure 9. *M–H* hysteresis loops measured at room temperature for: (a) Fe_3O_4-loaded CSs, (b) Fe_3O_4, and (c) $CoFe_2O_4$.

size, as can be seen from table 1, where the saturation magnetization increased with the increase of the particle size. Hence, increasing the particle size in Fe_3O_4 would result in fewer crystal defects and more homogenous particle shape [40]. Therefore, the super exchange interaction of Fe–O–Fe was strengthened, and the magnetic properties of Fe_3O_4 nanoparticles were better for the aqueous medium sample. However, it is interesting to note that remanence magnetization (M_r) and coercive force (H_c) of the two samples are inconspicuous, as shown in table 2. The very low H_c might be caused by the surface coordination of hydroxyl, which attached to the particle surfaces, thus altering the exchange interactions between the neighboring iron ions and eventually leading to a decrease in the remanence magnetization and coercive force of the magnetite particles. These data mean that the samples were in superparamagnetic state. However, it is clear that the value of saturation magnetization of $CoFe_2O_4$ is 36.1 emu/g, which is smaller than the bulk value (~80 emu/g) [41]. This result can be attributed to the nano-sized $CoFe_2O_4$ particles in which the surface areas are larger, and thus the surface energy and surface tension are high. This result changes in cationic preferences and led to an increased degree of anti-site defects and thus

Table 2. Crystallite size, average particle size, and magnetic properties of produced ferrites samples.

Sample	Crystallite size (nm)	Magnetic properties		
		Saturation magnetization M_s (emu/g)	Remanence magnetization M_r (emu/g)	Coercive field H_c (Oe)
Fe_3O_4-loaded CSs	50.0	48.9	1.2	12.0
Fe_3O_4	65	35.3	5.7	115.8
$CoFe_2O_4$	86	36.1	15.9	1189.9

lesser magnetization, i.e. the degree of inversion in $CoFe_2O_4$ in which there is exchange of Co^{2+} and Fe^{3+} ions from octahedral and tetrahedral sites and vice versa [42]. Compared with the H_c value of bulk $CoFe_2O_4$ reported in the literature (5400Oe), the produced $CoFe_2O_4$ nanocrystals exhibited smaller coercivity, which is likely attributed to their nanostructures [43, 44]. More detailed investigations on the magnetic properties of these products are still under way. The magnetic properties enable them to be manipulated easily by means of an external magnetic field. We believe that the magnetic composites obtained will have many important applications in advanced magnetic materials and biomedical fields, such as MRI, targeted drug delivery, and biomolecular detection and separations.

The above experimental results show that this synthesis strategy is simple, easy, and mild for preparing iron oxide-loaded functionalized CSs. Furthermore, it was also observed that the strategy has good reproducibility and the as-synthesized composites are highly air-stable. This strategy presents a novel pathway for the preparation of the composites. Thus, it can be concluded that Fc and its some derivatives can be used as precursors for the preparation of the iron oxide-loaded CSs. It is expected that this synthesis strategy may also be extended to other metallocenes or organometallic compounds for preparing other functional materials.

4. Conclusions

Size and surface-tunable CSs loaded with ferrites (Fe_3O_4-loaded CSs or $CoFe_2O_4$) nanoparticles. This is the first report on the one-step synthesis of these composites using acetylferrocene and its derivatives as precursor in the solvothermal system. The composites with many functional groups and magnetic nanoparticles on the surface of the CSs may not only make possible the loading of other functional molecules for diagnostics and drug delivery but also contribute to the development of multifunctional magnetic materials for applications in advanced magnetic materials and biomedical fields. Good saturation magnetization, 48.8 and 36.1emu/g, were achieved for the formed Fe_3O_4-loaded CSs and $CoFe_2O_4$, respectively. Further work on using the composites is in progress.

Acknowledgement

This work was supported by the Central Metallurgical Research and Development Institute (CRDI), Cairo, Egypt.

References

[1] Ph. Serp, R. Feurer, Ph. Kalck, Y. Kihn. JL. Faria, JL. Figueiredo, *Carbon*, **39**, 621 (2001).
[2] Q. Wang, F. Cao, Q. Chen, C. Chen. *Sol. Mater. Lett.*, **59**, 3738 (2005).
[3] H. Hou, A.K. Schaper, F. Weller, A. Greiner. *Chem. Mater.*, **14**, 3990 (2002).
[4] Z. Wang, L. Yu, W. Zhang, Z. Zhu, G. He, Y. Chen, G. Hu. *Phys. Lett.*, **A307**, 249 (2003).
[5] H. Li, Q. Wang, L. Shi, L. Chen, X. Huang. *Chem. Mater.*, **14**, 103 (2002).
[6] H. Li, Q. Wang, L. Shi, L. Chen, X. Huang. *Carbon*, **39**, 2211 (2001).
[7] X.L. Li, T.J. Lou, X.M. Sun, Y.D. Li. *Chemistry*, **43**, 5442 (2004).
[8] V.G. Pol, M. Motiei, A. Gedanken, J. Calderon-Moreno, Y. Mastai. *Chem. Mater.*, **15**, 1378 (2003).
[9] A.B. Fuertes, P. Tartaj. *Small*, **3**, 275 (2007).
[10] R. Li, H. Li, X. Qiu, L. Chen. *Chem. Eur. J.*, **12**, 4083 (2006).
[11] X. Hu, J.C. Yu, J. Gong. *J. Phys. Chem. C*, **111**, 11180 (2007).
[12] X. Sun, Y. Li. *Angew. Chem. Int. Ed.*, **43**, 597 (2004).
[13] Q. Wang, H. Li, L. Chen, X. Huang. *Carbon*, **39**, 2211 (2001).

[14] X. Wang, P. Hu, F. Yuan, L. Yu. *J. Phys. Chem. C*, **111**, 6706 (2007).
[15] M.S. Martina, J.P. Fortin, C. Menager, O. Clement, G. Barratt, C. Grabielle-Madelmont, F. Gazeau, V. Cabuil, S. Lesieur. *J Am. Chem. Soc.*, **127**, 10676 (2005).
[16] N.A. Frey, S. Peng, K. Cheng, S. Sun. *Chem. Soc. Rev.*, **38**, 2532 (2009).
[17] D. Yu, X. Sun, J. Zou, Z. Wang, F. Wang, K. Tang. *J. Phys. Chem. B*, **110**, 21667 (2006).
[18] Y. Sun, Y. Xia. *Science*, **298**, 2176 (2002).
[19] S.W. Cao, Y.J. Zhu, M.Y. Ma. L. Li, L. Zhang, *J. Phys. Chem. C*, **112**, 1851 (2008).
[20] Y. Zhu, W. Zhao, H. Chen, J. Shi. *J. Phys. Chem. C*, **111**, 5281 (2007).
[21] H. Deng, X. Li, Q. Peng, X. Wang, J. Chen, Y. Li. *Angew. Chem. Int. Ed.*, **44**, 2782 (2005).
[22] S.B. Cho, J.S. Noh, S.J. Park, D.Y. Lim, S.H. Choi. *J. Mater. Sci.*, **42**, 4877 (2007).
[23] G. Xi, C. Wang, X. Wang. *Eur. J. Inorg. Chem.*, **2008**, 425 (2008).
[24] L. Jing, Z. Hao, J. Shouheng Sun, L. Ping, W. Zhong Lin, *J. Phys. Chem*., **108**, 14005 (2004) .
[25] A.E.-H. Abdel-Nasser. *Carbon*, **41**, 713 (2003).
[26] I. Loa, C. M€oschel, A. Reich, W. Assenmacher, K. Syassen, M. Jansen. *Phys. Stat. Sol. (b)*, **223**, 293 (2001).
[27] N.T. Mc Devitt, W.L. Baun, *Spectrochim. Acta*, **20**, 799 (1964).
[28] C.J. Serna, M. Ocana, J. Iglesias. *J. Phys. C: Solid State Phys.*, **20**, 473 (1987).
[29] Z.H. Jing, S.H. Wu. *Mater. Chem. Phys.*, **92**, 600 (2005).
[30] R.M. Mohamed, M.M. Rashad, F.A. Haraz, W. Sigmund. *J. Magn. Magn. Mater.*, **322**, 2058 (2010).
[31] C. Yao, Y. Shin, L.Q. Wang Jr, C.F. Windisch, W.D. Samuels, B.W. Arey, et al. *J. Phys. Chem. C*, **111**, 15141 (2007).
[32] Y. Xia, B. Gates, Y. Yin, Y. Lu. *Adv. Mater.*, **12**, 693 (2000).
[33] Z. Yi, Y. Liang, X. Lei, C. Wang, J. Sun. *Mater. Lett.*, **61**, 4199 (2007).
[34] D. Peng, S. Beysen, Q. Li, J. Jian, Y. Sun, J. Jiwuer. *Particuology*, **7**, 35 (2009).
[35] L. Chen, Z. Lin, C. Zhao, Y. Zheng, Y. Zhou, H. Peng. *J. Alloys Compd.*, **509**, L1 (2011).
[36] C.Q. Hu, Z.H. Gao, X.R. Yang. *Chem. Phys. Lett.*, **429**, 513 (2006).
[37] T. Hosono, H. Takahashi, A. Fujita, R.J. Joseyphus, K. Tohji, B. Jeyadevan. *J. Magn. Magn. Mater.*, **321**, 3019 (2009).
[38] K. He, C.-Y. Xu, L. Zhen, W.-Z. Shao. *Mater. Lett.*, **61**, 3159 (2007).
[39] R.Y. Hong, T.T. Pan, H.Z. Li. *J. Magn. Magn. Mater.*, **303**, 60 (2006).
[40] S. Ni, X. Wang, G. Zhou, F. Yang, J. Wang, Q. Wang, D. He. *Mater. Lett.*, **63**, 2701 (2009).
[41] Z. Zi, Y. Sun, X. Zhu, Z. Yang, J. Dai, W. Song. *J. Magn. Magn. Mater.*, **321**, 1251 (2009).
[42] M.M. Rashad, R.M. Mohamed, H. El-Shall. *J. Mater. Process. Technol.*, **198**, 139 (2008).
[43] P.D. Thang, G. Rijnders, D.H.A. Blank. *J. Magn. Magn. Mater.*, **295**, 251 (2005).
[44] O.N. Shebanova, P.J. Lazor. *J. Raman Spectrosc.*, **34**, 845 (2003).